Human-centric Computing and Information Sciences

RESEARCH

Open Access

Feature extraction for robust physical activity recognition

Jiadong Zhu[1], Rubén San-Segundo[2*] and José M. Pardo[2]

*Correspondence: ruben.sansegundo@upm.es
[2] Speech Technology Group, E.T.S.I. Telecomunicación, Universidad Politécnica de Madrid, Ciudad Universitaria, Madrid 28040, Spain
Full list of author information is available at the end of the article

Abstract

This paper presents the development of a Human Activity Recognition (HAR) system that uses a network of nine inertial measurement units situated in different body parts. Every unit provides 3D (3-dimension) acceleration, 3D angular velocity, 3D magnetic field orientation, and 4D quaternions. This system identifies 33 different physical activities (walking, running, cycling, lateral elevation of arms, etc.). The system is composed of two main modules: a feature extractor for obtaining the most relevant characteristics from the inertial signals every second, and a machine learning algorithm for classifying between the different activities. This paper focuses on the feature extractor module, evaluating several types of features and proposing different normalization approaches. This paper also analyses the performance of every sensor included in the inertial measurement units. The main experiments have been done using a public available dataset named REALDISP Activity Recognition dataset. This dataset includes recordings from 17 subjects performing 33 different activities in three different scenarios. Final results demonstrate that the proposed HAR system significantly improves the classification accuracy compared to previous works on this dataset. For the best configuration, the system accuracy is 99.1%. This system has been also evaluated with the OPPORTUNITY dataset obtaining competitive results.

Keywords: Physical activity recognition, Human Activity Recognition, Feature extraction robustness, Type of sensor, Signal normalization, REALDISP Activity Recognition dataset, OPPORTUNITY dataset, Random Forest, Pattern recognition, Machine learning

Introduction

With information obtained from sensors, computer based system can make more intelligent actions by adapting their behavior to the context conditions. These days, thanks to the development of multi-sensor networks, related research areas have increased rapidly. Among those areas, Human Activity Recognition (HAR) based on wearable sensors (accelerometer, gyroscope, magnetometer, etc.) has recently received lots of attention due to its large number of promising applications. One of the most interesting HAR applications is ubiquitous identification of physical activity. As we know, over-weighting is a general human problem as a result of a physical inactivity habit. A Lancet publication [1] estimates that physical inactivity causes 9% of all premature deaths worldwide. By monitoring physical activity, we can help people to learn the calories they consumed or gained during the day in a much more precise way and

Springer Open

encourage them to keep moving in order to prevent obesity along with the following health effects. Another delightful example is Home Care Monitoring, which allows disabled and elderly patients a continuous health and well-being supervision while they perform Activities of Daily Living (ADL) at home. For instance, when a patient falls, the system will alert a nurse, or, if the patient is doing a forbidden activity, the security staff [2].

The main contributions of this paper are the followings:

- We present an automatic HAR system for classifying 33 different physical activities.
- We analyze several feature extraction strategies to find the one with the best performance and robustness.
- We study the influence of the type of sensor on the system performance.
- We propose and evaluate several normalization strategies for dealing with the inter-user variability.
- We also evaluate and validate the system for Home Care Monitoring using an ADL dataset.

The results obtained in this paper significantly improve the accuracy obtained in previous works on the same dataset.

This paper is organized as follows: Second section describes the background. Third section shows the system architecture in detail. Fourth section describes the dataset, the evaluation methods used in this work and the experimental results obtained with the proposed system. Sixth section summarizes the main conclusions.

Background

Human Activity Recognition systems can be categorized by machine learning algorithm and the type of sensor they used. Human activity recognition can be seen as a machine learning problem. To deal with this problem, the HAR system must extract features from sensor signals, generate a model for each activity, and classify next activities based on these models. In the literature, different machine learning solutions have been applied to the recognition of activities including Naive Bayes [3], Decision Trees [4], Support Vector Machines (SVMs) [5], Deep Neural Networks [6] and Hidden Markov Models (HMMs) [7]. In many works, several approaches have been compared using the WEKA learning toolkit [8] because it incorporates many machine learning algorithms. For example, Yang [9] compares the performance of several machine learning approaches: C4.5 Decision Trees, Naive Bayes, k-Nearest Neighbor, and Support Vector Machines. Kwapisz [10] compares three learning algorithms: logistic regression, J48, and multilayer perceptron. Not only supervised but also, unsupervised algorithms have been studied [11]. In many works [12], complex algorithms, like the Random Forest, have demonstrated a very good performance compared to simple classification algorithms. Because of this, the Random Forest has been the algorithm selected in this work.

For HAR, there are two main types of sensors: ambient and on-body sensors. In terms of ambient sensors, the most widely used sensors are video cameras [13]. Video recording is one of the main strategies for supervising human behavior and activities [14]. But, this behavior can also be studied by analyzing acoustic events. The human activity can be characterized by defining the identity of sounds and their position in time sequence [15]. The main two disadvantages of ambient sensors are the requirement of infrastructure (for example, installation of video cameras in the monitoring areas) and also, people do not always stay all their time in the same environment. These limitations can be overtaken by on-body sensors [16, 17]. Body-worn sensors add new possibilities to the human monitoring system [18]: they allow measuring body signals (e.g. physiological, motion, location) and they are portable, allowing user supervision at any location without the need of fixed infrastructure. Because of these benefits, several works have been developed using motion sensors in different body parts (e.g. waist, wrist, chest and thighs) and achieved good classification performance [19–22].

This work has been carried out using a public dataset: REALDISP Activity Recognition dataset. This dataset contains recordings from 17 subjects performing 33 different gymnastic activities. This dataset has permitted several HAR works focused on different aspects. One interesting aspect has been the degradation suffered on the HAR accuracy depending on the sensor placement or the number of displacements (wrong placements) [23–25]. Other analyzed aspects have been the window size [24, 26], and the detection of activities transitions [27]. This paper contributes by analyzing several strategies for feature extraction and proposing several normalization approaches for dealing with the inter-user variability. As far as the authors know, this work reports the best HAR results using this dataset.

System architecture

The proposed system architecture is shown in Fig. 1. It consists of two main modules: feature extraction and machine learning algorithm for activity classification. The inertial signals are recorded by 9 inertial measurement units. Every unit contains four sensors, accelerometer (ACC), gyroscope (GYR), magnetometer (MAG) and quaternion (QUAD)

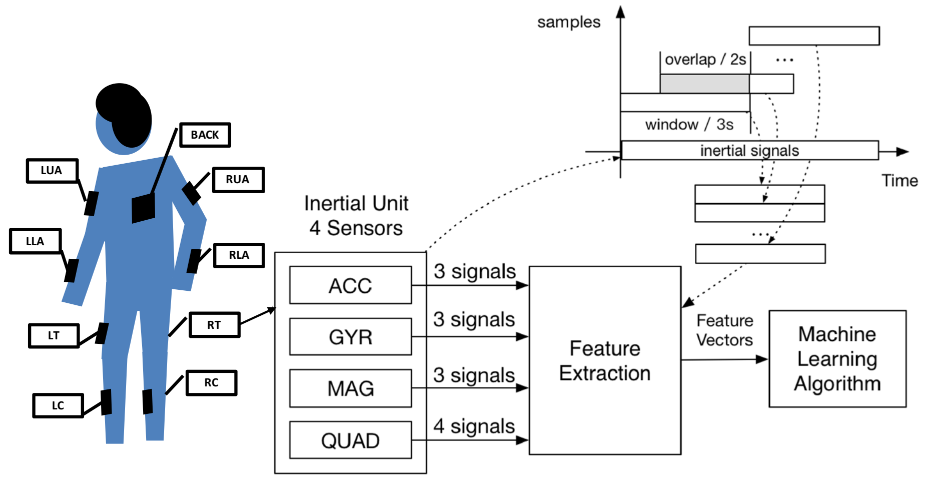

Fig. 1 System architecture (the sensor placement is referenced from [24]). The system architecture includes two steps: feature extraction and activity classification. This system includes 9 inertial measurement units generating and every unit contains four sensors, accelerometer (ACC), gyroscope (GYR), magnetometer (MAG) and quaternion (QUAD) sensor

sensor, which generate 13 inertial signals: in total, 117 inertial signals are processed. For more details, the reader can refer to [24].

Feature extraction

In the feature extraction module, the sample sequences from the inertial signals are grouped together in frames: fixed-width sliding windows of 3 s and 66% overlap (150 samples per frame with an overlap of 100 samples). For each frame, the system calculates a feature vector, which makes it easier for the machine learning module to learn the internal characteristics behind raw signals. These features are traditional measures like the mean, correlation, Signal Magnitude Area (SMA) and auto regression coefficients, but also, advanced ones that will be described below. These features are computed from 117 signals obtained from nine measurement units. Taking the three accelerometer signals (X, Y, Z) as an example (similar signals are also considered for gyroscope, magnetometer and quaternion sensor): in the time domain, the signals considered in this work are:

- XYZ (3 signals): Original accelerometer signals.
- Mag (1 signal): Magnitude signal computed from the previous three signals. This magnitude is computed as the square root of the sum of squared components (accelerometer signals).
- Jerk-XYZ (3 signals): Jerk signals (derivative of the accelerometer signals) obtained from the original accelerometer signals.
- JerkMag (1 signal): Magnitude signal computed from the previous jerk signals (square root of the sum of squared components).

And in the frequency domain, the signals from the accelerometer sensor are:

- fXYZ (3 signals): Fast Fourier transforms (FFTs) from XYZ.
- fMag (1 signal): FFT from Mag.
- fJerk-XYZ (3 signals): FFTs from Jerk-XYZ.
- fJerkMag (1 signal): FFTs from JerkMag.

The set of features that were estimated from the time domain signals are:

- Mean value, standard deviation, median absolute deviation, minimum and maximum values of the samples in a frame.
- Signal Magnitude Area: The normalized integral of the samples in a frame.
- Energy measure: Sum of the squares samples divided by the number of samples in a frame.
- Inter-quartile range: Variability measure obtained by dividing a data set into quartiles.
- Signal entropy.
- Auto-regression coefficients with Burg order equal to four correlation coefficients between two signals.

The set of features estimated from frequency domain signals include similar features to those from the time domain, plus:

- Index of the frequency component with largest magnitude.
- Weighted average of the frequency components to obtain a mean frequency.
- Skewness and Kurtosis of the frequency domain signal.
- Energy of 6 equally spaced frequency bands within the 64 bins of the FFT.

Regarding the feature extraction complexity, we can comment that every feature is represented by 4 bytes, so every frame needs around 16 kB for storing a feature vector with all the features (4086 features) from all signals (117 signals from 9 measurement units). The features extractor has been implemented using Octave v.4.0.1. This module needs 12 min. for extracting the features in a whole session (around 18 min of physical exercise) using an Intel Core I7-4790 CPU at 3.6 GHz with 16 GB of RAM.

Machine learning algorithm

The machine learning algorithm module acts as a classifier. For this module, we have tried two popular algorithms (J48 decision tree and Random Forest) and found that the Random Forest algorithm [28] works better in this circumstance. In our preliminary experiments, it defeats the J48 decision tree algorithm by nearly 10% in accuracy. Therefore, the Random Forest algorithm is used in our following experiments.

The Random Forest algorithm creates several decision trees during training. In our experiments, the number of trees ranges from 40 to 95, and the number of nodes per tree goes from 15 to 87. These numbers varies strongly with the number of features considered in the feature extractor. The algorithm for training the Random Forest model is:

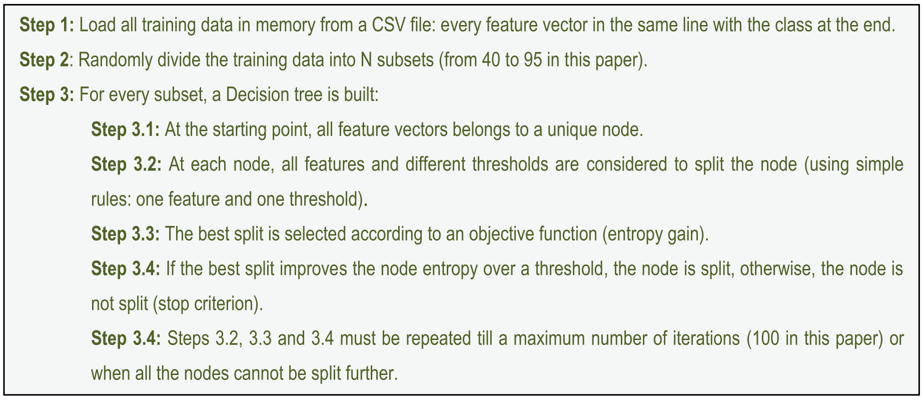

```
Step 1: Load all training data in memory from a CSV file: every feature vector in the same line with the class at the end.
Step 2: Randomly divide the training data into N subsets (from 40 to 95 in this paper).
Step 3: For every subset, a Decision tree is built:
        Step 3.1: At the starting point, all feature vectors belongs to a unique node.
        Step 3.2: At each node, all features and different thresholds are considered to split the node (using simple rules: one feature and one threshold).
        Step 3.3: The best split is selected according to an objective function (entropy gain).
        Step 3.4: If the best split improves the node entropy over a threshold, the node is split, otherwise, the node is not split (stop criterion).
        Step 3.4: Steps 3.2, 3.3 and 3.4 must be repeated till a maximum number of iterations (100 in this paper) or when all the nodes cannot be split further.
```

Regarding the algorithm complexity, for building every decision tree the time complexity is $\mathrm{O(m \cdot n \cdot log(n))}$, where n is the number of feature vectors in the training set, and m is the number of features in every feature vector. For building all the decision trees, the time complexity is $\mathrm{O(t \cdot m \cdot n \cdot log(n))}$, where t is the number of decision trees considered in the model.

For classification, every new input from the testing set is run down all of the trees. The classification result is weighted average of all of the terminal nodes that are reached, providing the final decision:

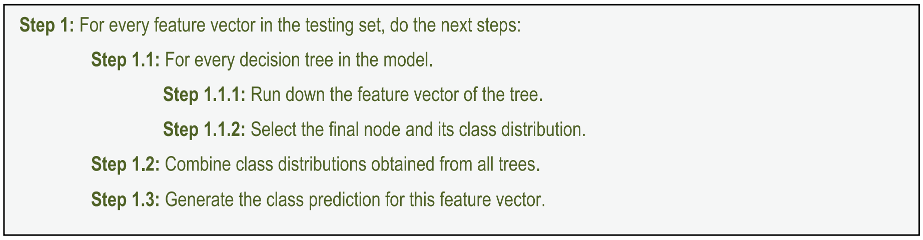

```
Step 1: For every feature vector in the testing set, do the next steps:
    Step 1.1: For every decision tree in the model.
        Step 1.1.1: Run down the feature vector of the tree.
        Step 1.1.2: Select the final node and its class distribution.
    Step 1.2: Combine class distributions obtained from all trees.
    Step 1.3: Generate the class prediction for this feature vector.
```

For testing, the time complexity is O(t · n · m), where *n* is the number of feature vectors in the testing set, *m* is the number of features in every feature vector, and *t* is the number of decision trees considered in the model.

This work has been carried out using the Random Forest implementation included in the WEKA toolkit [8] (weka configuration weka.classifiers.trees.randomforest -I 100 -K 0 -S 1).

The training process needs less than 10 min for training the system using 16 sessions. The analysis and evaluation of 1 session (around 18 min of physical exercise) need less than 60 s, using an Intel Core I7-4790 CPU at 3.6 GHz with 16 GB of RAM.

Experiments

This section describes the experiments conducted in this work. In first and second subsection, the main dataset and the evaluation methods used in this work are introduced. Third and fourth subsections shown the experiments carried out for the analysis of the type of sensor and the type of feature. In fifth subsection, the final results on the main dataset are given. At the end, sixth subsection includes an additional experiment on another HAR dataset—OPPORTUNITY dataset, using the same system.

REALDISP dataset

In this work, the HAR system has been mainly trained and tested using the REALDISP Activity Recognition dataset, available at the UCI Machine Learning Repository [24]. This dataset includes recordings from 17 subjects, seven females and ten males, with ages ranging from 22 to 37 years old. These recording include 13 inertial signals obtained from 9 on-body inertial measurement units located on different body parts. Each unit contains four sensors: an accelerometer, a gyroscope, a magnetometer and a quaternion sensor. Using these sensors, a 3D (3-dimension) linear acceleration, a 3D angular velocity, a 3D magnetic field orientation and a 4D quaternions are sampled every 20 ms (50 Hz sample-rate). The experiment consisted in performing a complete set of exercises: 33 physical activities, including warm up, fitness and cool down activities (walking, jogging, cycling, jumping, etc.). One run-through of the exercises lasted 15–20 min. Each session was preceded by a preparation phase lasting around 30 min. This dataset also includes a Null-activity. This label has been assigned to other activities (different from the 33 activities considered in this study), and also, the transitions between activities.

The most significant characteristic of this dataset is the introduction of sensor displacement, such as rotation and mis-positioning from the corresponding body part. The dataset includes recordings in three placement scenarios:

- *Ideal-placement* all sensors were placed by experts at their optimal place for classification. All the subjects recorded a session in these conditions (17 sessions).
- *Self-placement* every subject decides the positions of three sensors by themselves and the remaining sensors were situated by experts. The number of three is considered a reasonable estimate of the proportion of sensors that may be misplaced during the normal wearing. All the subjects recorded a session in these conditions (17 sessions).
- *Mutual-placement* where several displacements were intentionally introduced by experts. Three out of the 17 volunteers were recorded for mutual-displacement scenario (subjects 2, 5 and 15). These three subjects recorded one session for every sensor configuration: for the case in which four, five, six or even seven out of the nine sensors are misplaced.

Considering the size, the number of activities and the different placement scenarios, we think that the REALDISP dataset is an appropriate dataset to evaluate the performance of the proposed HAR system.

Evaluation methods

In this work, we apply two methods to evaluate the system performance. The first one is a tenfold random-partitioning cross-validation evaluation. This method consists of splitting the whole database (with all subjects' data) randomly into 10 equal parts (subsets). For every experiment, one subset is used for testing and the other nine for training, considering a round-robin strategy. The final cross-validation result is the average along the 10 experiments. This is the method used in the original paper [24].

However, our hypothesis is that this method suffers the problem that the data in both training and testing could contain information from a same subject, so the machine learning algorithm can learn not only physical activity characteristics but also some subject-dependent ones. This aspect makes it hard to evaluate the system performance when facing a new subject. In order to verify this hypothesis, sect. "Evaluation methods" includes some experiments comparing both evaluation methods.

Therefore, we propose the second method, a subject-wise cross-validation. In this case, the same kind of cross-validation is done but on different subjects rather on automatically split parts: all data from the same user is considered for testing and the data from the remaining subjects for training. Since we have 17 subjects in the database, this experiment is repeated 17 times. The final experimental result is the average of accuracy and F-measure on all 17 sub-experiments weighted by the number of samples in every testing data.

In this work, we only use the tenfold cross-validation method to compare with our second evaluation method ("Evaluation methods"). The rest experiments are conducted with the subject-wise method.

In order to measure the statistical significance of the improvements, we apply the concept of Confidence Interval defined by Eq. 1 [29], P is the accuracy rate, and N is the amount of instances in the data set: more than 130,000 in the REALDISP dataset.

$$\delta = \pm 1.96 \times \sqrt{\frac{P(100 - P)}{N}} \tag{1}$$

If the accuracy difference between two experiments is bigger than the confidence interval, this difference can be considered significant with a 95% of probability. In this paper, for all the experiments, the confidence interval is lower than 0.5%, so any difference higher than this value, this difference can be considered as significant with a 95% a probability.

Data analysis

In this section, we first conduct some experiments for HAR system configuration tuning in order to analyze how the evaluation, the sensor type, or the feature type influences the system performance.

Evaluation method

This section includes the experiments considering the two different evaluation methods. In these experiments, the setup is: ideal-placement, Null-activity removed (as in the original paper), and time-based features. The experimental results are shown in Table 1. From the results, we can clearly see that the result given by the random-partitioning method is significantly better than the subject-wise method: the accuracy (Acc%) difference is 3.4% (99.1–95.5%) higher than the confidence interval, 0.5%.

This result supports the hypothesis stated in the previous section: in the random-part evaluation, training and testing subsets could contain information from a same subject and this characteristic produces better classification results. In the rest of the paper, we will only consider the subject-wise evaluation method (more challenging situation).

Type of sensor

This section includes the experiments on different sensor types. In these experiments, the setup is: ideal-placement, Null-activity removed (as in the original paper), and time-based features. The experimental results are shown in Table 2. From the results, we can clearly see that the 3D magnetometer works best among the four types of sensor and the quaternion sensor performs the worst. The accuracy (Acc%) differences are statistically relevant because they are bigger than the confidence interval (0.5%).

Table 1 Experimental results depending on the evaluation method

Sensor	Evaluation	# of features	Acc%	F-measure
ACC	Random-part	954	99.1	0.991
ACC	Subject-wise	954	95.5	0.951

Table 2 Experimental results on type of sensor

Sensor	Evaluation	# of features	Acc%	F-measure
ACC	Subject-wise	954	95.5	0.951
GYR	Subject-wise	954	94.4	0.941
MAG	Subject-wise	954	*96.3*	*0.952*
QUAD	Subject-wise	1224	93.0	0.924

Italic values indicate the best results in this experiment

Type of feature

We also make a comparison on the performance of different kinds of features, more specifically, temporal features and frequency features as described in "Feature extraction". Same as the experiments on sensor types, here, we also consider the ideal-placement, removing the Null-activity. For the sake of confidence, we repeat the experiments with different types of sensor.

From the results shown in Fig. 2, it is obvious that the temporal features always beat the frequency features and their combination in the cases of all three sensor types. Therefore, we consider only the time-based features in the rest experiments.

As a conclusion, it is clear that using the signals from magnetometer and the time-based features is currently the best system configuration. By including all sensors, we obtain even higher system accuracy: 97.0%.

Normalization methods

When training and testing with different subjects, it is important to deal with the inter-user variability. In order to reduce this variability, we propose several normalization strategies. In this work, we evaluate six normalization methods, considering two different places where this normalization is applied: before and after the feature extraction.

1. Mean removal: Subtract the mean value from each value in a feature or signal vector.
2. Z-Score: Mean removal first, and divide each value by its standard deviation.
3. Histogram equalization: Consider all the values in a gray-scale, and equalize its histogram.
4. 0–1 mapping: Distribute all data to the 0–1 range.
5. Vector normalization: Divide each value in a vector with the vector's magnitude.
6. Vector normalization with mean normalization: Vector normalization followed by mean removal.

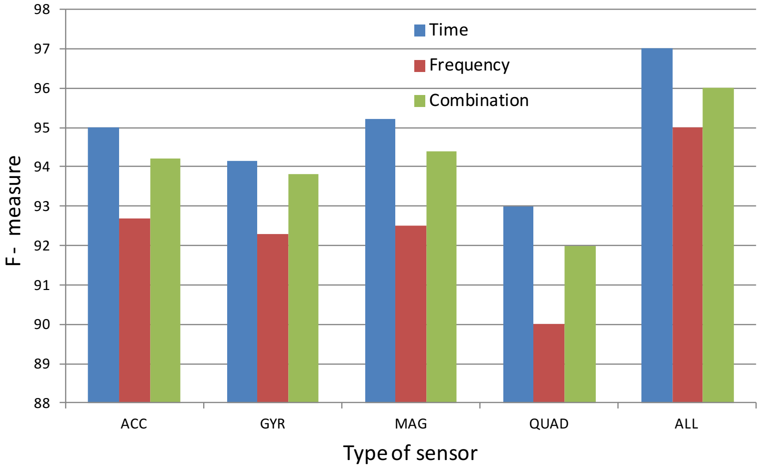

Fig. 2 Experimental results on type of feature. This figure represents and compares the results for different kinds of features: temporal features and frequency features and using different types of sensors

Table 3 Experimental results on normalization methods

Method	ACC		GYR		MAG		QUAD	
	Acc%	F-measure	Acc%	F-measure	Acc%	F-measure	Acc%	F-measure
None	95.5	0.951	94.4	0.941	96.3	0.952	93.0	0.924
SIGN 1	94.7	0.943	93.6	0.935	96.1	0.957	92.2	0.923
SIGN 2	94.5	0.938	93.6	0.929	93.4	0.924	92.1	0.923
SIGN 3	89.2	0.880	88.1	0.870	93.6	0.927	87.5	0.865
SIGN 4	92.7	0.920	91.5	0.910	94.0	0.931	90.8	0.901
SIGN 5	*96.4*	*0.961*	*95.4*	*0.950*	*97.9*	*0.976*	*94.1*	*0.939*
SIGN 6	96.1	0.958	95.1	0.949	94.8	0.943	93.8	0.934
FEAT 1	95.6	0.951	94.5	0.940	95.6	0.950	93.0	0.930
FEAT 2	95.4	0.948	94.3	0.937	95.2	0.946	93.1	0.925
FEAT 3	94.7	0.940	93.5	0.932	95.0	0.944	92.1	0.920
FEAT 4	94.8	0.943	93.6	0.932	95.8	0.954	92.3	0.921
FEAT 5	92.2	0.916	91.1	0.908	96.4	0.960	90.2	0.892
FEAT 6	93.9	0.932	94.8	0.926	96.1	0.956	91.5	0.910

Italic values indicate the best results in this experiment

Note that in Table 3, SIGN_1 means normalization on signal data using method 1 and FEAT_1 means normalization on feature data (i.e. after feature extraction) using method 1. The results show that the vector normalization method (number 5) applied directly on the signal data outperforms all other methods. Thus, for the rest of the report, we use this normalization method before the feature extraction.

Final results and discussion

By applying the best experimental configuration described above, we conducted experiments using data from all signals and all sensors in all the three placement scenarios.

Ideal placement

Table 4 shows our final experimental results for the ideal placement scenario. After introducing the signal normalization method and considering all sensors, the system accuracy goes to 99.4%, a 2.4% improvement compared to the original paper (97%). This improvement is higher than the confidence interval (0.5%) so the difference is statistically significant with a 95% of probability. It is important to notice that, in the original paper, the evaluation method was random-partitioning and, based on the results presented in "Evaluation method", the baseline accuracy would be even lower when using the subject-wise cross-validation method.

Another aspect to comment is regarding the Null-activity. In the first two rows of Table 4, the experiments are conducted without considering the Null-activity, in other words, it is a 33-class classification task. We truncated the Null-activity samples in order to make a fair comparison with the original paper. In this work, we have also done experiments including the Null-activity, which, in our opinion, is closer to a real situation. So, the problem now becomes more challenging: a 34-class classification task. Regarding the results shown in the third row of Table 4, our system still maintains a high performance when the Null-activity is included: the system only loses 0.3% accuracy (from 99.4 to 99.1%) showing a significant improvement (2.1%) respect to the baseline system (97%).

Table 4 Final experimental results considering the ideal placement scenario

System	Accuracy %	F-measure
Baseline [24]: Evaluation method: random-partitioning Null-activity: truncated	97.0	–
This paper: Evaluation method: subject-wise Null-activity: truncated	99.4	0.993
This paper: Evaluation method: subject-wise Null-activity: included	99.1	0.991

Such low degradation is made possible due to the large number of features extracted and the suitable normalization method proposed in this paper.

Self and mutual placement

We repeat the previous experiments on the other two scenarios described in "REALDISP dataset": self-placement and mutual-placement. The results are presented in Table 5. In the first two columns, this table shows the type of data (or scenario where the data were recorded) used for training and testing the proposed system.

Regarding the self-placement scenario, this table shows 8.6% accuracy drop compared to the ideal-placement in the original paper (from 97.0 to 88.4%), but with our system, this reduction is lower than 0.5% (from 99.1 to 98.9%). When comparing these results to the original paper, there is a big improvement (more than 10%, from 88.4 to 98.9%) in the self-placement scenario. The new feature extraction module shows a very good robustness against different sensor placements.

For the mutual-placement scenario, the results are considerably low in both works (baseline and this paper) but the degradation obtained with the system proposed in this paper is considerably smaller compared to the baseline system: our system shows a better robustness. This degradation is different depending on the number of mis-displacements (4, 5, 6, and 7).

In these experiments, we have used the data recorded in the mutual scenario for training and testing the system. As we commented in "REALDISP dataset", only three out of the 17 volunteers were recorded for mutual-displacement scenario so the amount of data

Table 5 Final experimental result for self-placement and mutual-placement scenarios

Train set	Test set	Baseline [24]: Evaluation method: random-partitioning Null-activity: truncated		This paper: Evaluation method: subject-wise Null-activity: included	
		Accuracy %	F-measure	Accuracy %	F-measure
Ideal	Ideal	97.0	–	99.1	0.991
Self	Self	88.4	–	98.9	0.988
Mutual4	Mutual4	71.2	–	87.9	0.847
Mutual5	Mutual5	71.6	–	93.5	0.921
Mutual6	Mutual6	77.2	–	96.4	0.959
Mutual7	Mutual7	68.0	–	83.2	0.799

for training the system is very small (2 out of the 3 subjects recorded in this scenario). In order to analyze the influence of the amount of data, we repeat the same experiments but using the ideal-placement data for training the system. Although there is a mismatch in the conditions, the amount of available data for training would increase a lot (from 2 to 16 subjects). The experiments are shown in Table 6. In the "Train Set" and "Test Set" columns, we have also included the number of subjects considered for training and testing the system.

The results show that when being trained with ideal datasets and tested with mutual datasets, the system reaches a very good accuracy though the training and testing sets come from different placement scenarios. For example, for mutual4, the accuracy goes from 87.9 to 99.0% (the first row). These results support the hypothesis that the amount of data for training is an important factor in the system performance.

With the idea of cross-dataset experiment, we go further on the ideal-placement and self-placement scenarios (the last row in Table 6). As Table 6 shows, there is not a significant difference on the accuracy when testing with self-placement dataset and training with ideal or self placement (99.1 vs. 98.9%, difference lower than the confidence interval 0.5%). In this case, the amount of data available in ideal-placement and self-placement scenarios is the same.

System analysis in a new domain: home care monitoring

In the introduction, we commented two main applications of HAR: physical exercise monitoring and home care monitoring. The REALDISP dataset is focused on the first one: physical exercise monitoring. In order to verify the viability of the proposed system in a home care monitoring application, we have evaluated the best system configuration with another dataset: the OPPORTUNITY dataset for HAR from wearable, object, and ambient sensors [30]. The recordings include daily morning activities: getting up from the bed, preparing and having breakfast (a coffee and a salami sandwich) and cleaning the kitchen latter. This dataset is a very popular HAR dataset on this research field. There is no constraining on the location or body posture in any of the scripted activities.

Table 6 Final experimental result for self-placement and mutual-placement scenarios: using ideal-placement for training

This paper:
Evaluation method: subject-wise
Null-activity: included

Train set	Test set	Accuracy %	F-measure	Train set	Test set	Accuracy %	F-measure
Mutual4 (2 subjects)	Mutual4 (1 subject)	87.9	0.847	Ideal (16 subjects)	Mutual4 (1 subject)	99.0	0.990
Mutual5 (2 subjects)	Mutual5 (1 subject)	93.5	0.921	Ideal (16 subjects)	Mutual5 (1 subject)	98.1	0.982
Mutual6 (2 subjects)	Mutual6 (1 subject)	96.4	0.959	Ideal (16 subjects)	Mutual6 (1 subject)	99.0	0.990
Mutual7 (2 subjects)	Mutual7 (1 subject)	83.2	0.799	Ideal (16 subjects)	Mutual7 (1 subject)	94.5	0.938
Self (16 subjects)	Self (1 subject)	98.9	0.988	Ideal (16 subjects)	Self (1 subject)	98.9	0.989

OPPORTUNITY dataset

The OPPORTUNITY dataset contains data from four subjects, performing six different runs each of: ADL1–ADL5 and Drill. In the Drill run, subject must act in a predetermined activity sequence and, as for ADL1–ADL5, there is no restriction on the order and number of activities. For each subject, there is information from three types of sensors: body-worn sensors, object sensors and ambient sensors. The on-body sensors include 7 multi-sensor inertial measurement units with another 12 3D acceleration sensors: 145 signals in total. Since only body-worn sensors are concerned in the evaluation section of the original paper [31], the data from object and ambient sensors are truncated in the following experiments. In terms of activities or classes, this dataset has 3 different sets: 4 types of locomotion (high-level activities); 17 types of gesture (mid-level actions); and low-level actions to objects (which is ignored in this work).

Experiments on the OPPORTUNITY dataset

We retrain and evaluate our system using the same experimental setting as in the original paper [31]: using ADL2 and ADL3 from one subject as the testing set and use Drill, ADL1, ADL4 and ADL5 from the same subject as the training set. We conduct experiments in this configuration for all four subjects and in the two tasks: high-level locomotion (Table 7) and mid-level gestures (Table 8). The first column shows the different proposed systems, and the best systems are remarked with bold font.

For the high-level locomotion task (Table 7), the system proposed in this paper obtains the best results for all subjects when the Null class is not considered (the 4 last columns). When including the Null class (the 4 first columns), we obtain the best results for all subjects except S3.

For the mid-level gesture task (Table 8), the system proposed in this paper obtains the best results for all subjects except S4 when the Null class is included (the 4 first

Table 7 Experimental results on the OPPORTUNITY dataset (high-level locomotion classification)

Method	F-measure				F-measure (no null class)			
	S1	S2	S3	S4	S1	S2	S3	S4
Results from [31]								
LDA	0.62	0.64	0.68	0.43	0.73	0.70	0.74	0.53
QDA	0.67	0.66	0.71	0.45	0.81	0.77	0.79	0.56
NCC	0.60	0.58	0.56	0.45	0.69	0.67	0.62	0.50
1 NN	0.84	0.85	*0.83*	0.76	0.85	0.85	0.85	0.76
3 NN	0.85	0.86	*0.83*	0.77	0.86	0.86	0.85	0.76
UP		0.58	0.62			0.88	0.80	
NStar		0.58	0.66			0.88	0.85	
SStar		0.61	0.68			0.87	0.83	
CStar		0.60	0.65			0.90	0.83	
NU		0.54	0.49			0.83	0.63	
MI		0.85	0.81			0.87	0.86	
MU		0.57	0.68			0.86	0.87	
UT		0.48	0.55			0.74	0.72	
This paper	*0.88*	*0.88*	0.80	*0.85*	*0.92*	*0.92*	*0.89*	*0.86*

Italic values indicate the best results in this experiment

Table 8 Experimental results on the OPPORTUNITY dataset (mid-level gesture classification)

Method	F-measure				F-measure (no Null class)			
	S1	S2	S3	S4	S1	S2	S3	S4
Results from [31]								
LDA	0.65	0.63	0.70	0.62	0.36	0.28	0.27	0.17
QDA	0.60	0.57	0.69	0.64	0.34	0.29	0.34	0.22
NCC	0.48	0.48	0.51	0.35	0.29	0.21	0.22	0.14
1 NN	0.85	*0.89*	0.86	0.84	0.56	0.53	0.58	0.46
3 NN	0.85	*0.89*	0.86	*0.88*	0.55	0.53	0.58	0.48
NStar		0.84	0.83			0.60	0.69	
SStar		0.87	0.84			0.65	0.72	
CStar		0.88	*0.87*			*0.72*	*0.80*	
UP		0.64	0.64	0.64		0.23	0.19	0.16
NAGS				0.71				0.17
This paper	*0.87*	*0.89*	*0.87*	0.85	*0.76*	0.64	0.64	*0.55*

Italic values indicate the best results in this experiment

columns). In conclusion, the proposed system is also a competitive solution for home care monitoring applications.

Conclusions

This paper has proposed a HAR system for classifying 33 different physical activities composed of two main modules: feature extraction and activity recognition modules.

The first contribution has been an analysis of several feature extraction strategies: time-based and frequency-based. The time-based features have provided better results compared to the frequency-based ones. This paper has also evaluated several normalization methods for reducing the degradation produced when training and testing with different users. Thanks to the new feature extraction module and the normalization strategy, the system has shown strong robustness when facing the Null-activity and different placement scenarios, two vital aspects for real applications.

Regarding the type of sensor, the magnetometer signals have provided better discrimination capability. The best results have been obtained when combining the information from all the sensors. In this case, the improvement is significant. The main experiments have been done on a public available dataset, REALDISP Activity Recognition dataset. Final results have exhibited that the proposed system largely improves the performance compared to previous works on the same dataset [24]. Under the best configuration, the accuracy reaches 99.1% and F-measure 0.991.

The proposed system has been also evaluated with another public dataset (OPPORTUNITY dataset) demonstrating competitive results (compared to previous work [31]) in two main tasks for home care monitoring: high-level locomotion and mid-level gesture classification.

Abbreviations

3D: 3-dimension; ACC: accelerometer; ADL: Activities of Daily Living; GYR: gyroscope; HAR: Human Activity Recognition; HMM: Hidden Markov Model; MAG: magnetometer; QUAD: quaternion; SMA: Signal Magnitude Area; SVMs: Support Vector Machines.

Authors' contributions

JZ has implemented the HAR and executed the experimental work. RSS has conceptualized the HAR system, supervised the experiments and revised the manuscript. JMP analyzed the results, provided feedback and revised the final manuscript. All authors read and approved the final manuscript.

Author details

[1] School of Computer Science, Beijing University of Posts and Telecommunications, 10 Xitucheng Rd., Beijing 100876, China. [2] Speech Technology Group, E.T.S.I. Telecomunicación, Universidad Politécnica de Madrid, Ciudad Universitaria, Madrid 28040, Spain.

Acknowledgements

The authors would like to thank the UCI Machine Learning Repository and the researchers who kept the records and developed the REALDISP and OPPORTUNITY datasets.

Competing interests

The authors declare that they have no competing interests.

Availability of data and materials

The datasets supporting the conclusions of this article are available in the UCI Machine Learning Repository, https://archive.ics.uci.edu/ml/datasets.html. Regarding the software, the toolkit used for these experiments is WEKA (http://www.cs.waikato.ac.nz/ml/weka/). This tool has been developed in Java for multi platform use. Weka is open-source software issued under the GNU General Public License.

Funding

This work has been supported by China Scholarship Council scholarship and ASLP-MULÁN (TIN2014-54288-C4-1-R) and NAVEGABLE (MICINN, DPI2014-53525-C3-2-R) projects.

Publisher's Note

Springer Nature remains neutral with regard to jurisdictional claims in published maps and institutional affiliations.

Received: 15 November 2016 Accepted: 19 April 2017
Published online: 02 June 2017

References

1. Lee IM, Shiroma EJ, Lobelo F, Puska P, Blair SN, Katzmarzyk PT, Lancet Physical Activity Series Working Group et al (2012) Effect of physical inactivity on major noncommunicable diseases worldwide: an analysis of burden of disease and life expectancy. Lancet 380:219–229
2. Pavón J, Gómez-Sanz J, Fernández-Caballero A, Valencia-Jiménez JJ (2007) Development of intelligent multisensor surveillance systems with agents. Robot Auton Syst 55:892–903
3. Jatoba LC, Grossmann U, Kunze C, Ottenbacher J, Stork W (2008) Context-aware mobile health monitoring: evaluation of different pattern recognition methods for classification of physical activity. In: 2008 30th annual international conference of the IEEE engineering in medicine and biology society. IEEE, New York, pp 5250–5253
4. Maurer U, Smailagic A, Siewiorek DP, Deisher M (2006) Activity recognition and monitoring using multiple sensors on different body positions. In: International workshop on wearable and implantable body sensor networks (BSN'06). IEEE, New York
5. Anguita D, Ghio A, Oneto L, Parra X, Reyes-Ortiz JL (2013) Energy efficient smartphone-based activity recognition using fixed-point arithmetic. J UCS 19:1295–1314
6. Ronao CA, Cho S (2016) Human activity recognition with smartphone sensors using deep learning neural networks. Expert Syst Appl 59:235–244
7. San-Segundo R, Lorenzo-Trueba J, Martínez-González B, Pardo JM (2016) Segmenting human activities based on HMMs using smartphone inertial sensors. Pervasive Mob Comput 30:84–96
8. Holmes G, Donkin A, Witten IH (1994) Weka: a machine learning workbench. In: Proceedings of the 1994 Second Australian and New Zealand conference on intelligent information systems. IEEE, New York, pp 357–361
9. Yang J (2009) Toward physical activity diary: motion recognition using simple acceleration features with mobile phones. In: Proceedings of the 1st international workshop on Interactive multimedia for consumer electronics. ACM, New York, pp 1–10
10. Kwapisz JR, Weiss GM, Moore SA (2011) Activity recognition using cell phone accelerometers. ACM SIGKDD Explor Newsl 12:74–82
11. Kwon Y, Kang K, Bae C (2014) Unsupervised learning for human activity recognition using smartphone sensors. Expert Syst Appl 41(14):6067–6074
12. Stisen A, Blunck H, Bhattacharya S, Prentow TS, Kjærgaard MB, Dey A, Sonne T, Jensen MM (2015) Smart devices are different: assessing and mitigating mobile sensing heterogeneities for activity recognition. In: Proceedings of the 13th ACM conference on embedded networked sensor systems. ACM, New York, pp 127–140
13. Poppe R (2010) A survey on vision-based human action recognition. Image Vis Comput 28:976–990
14. Onofri L, Soda P, Pechenizkiy M, Iannello G (2016) A survey on using domain and contextual knowledge for human activity recognition in video streams. Expert Syst Appl 63(30):97–111
15. Temko A, Nadeu C, Macho D, Malkin R, Zieger C, Omologo M (2009) Chapter 7: Acoustic event detection and classification. In: Waibel A, Stiefelhagen R (eds) Computers in the human interaction loop. Springer, London, pp 61–73

16. Lukowicz P, Ward JA, Junker H, Stäger M, Tröster G, Atrash A, Starner T (2004) Recognizing workshop activity using body worn microphones and accelerometers. In: International conference on pervasive computing. Springer, Heidelberg, pp 18–32
17. Karantonis DM, Narayanan MR, Mathie M, Lovell NH, Celler BG (2006) Implementation of a real-time human movement classifier using a triaxial accelerometer for ambulatory monitoring. IEEE Trans Inf Technol Biomed 10:156–167
18. Bao L, Intille SS (2004) Activity recognition from user-annotated acceleration data. In: International conference on pervasive computing. Springer, Heidelberg, pp 1–17
19. Casale P, Pujol O, Radeva P (2011) Human activity recognition from accelerometer data using a wearable device. In: Iberian conference on pattern recognition and image analysis. Springer, Heidelberg, pp 289–296
20. Krishnan NC, Colbry D, Juillard C, Panchanathan S (2008) Real time human activity recognition using tri-axial accelerometers. Sensors, signals and information processing workshop. pp 3337–3340
21. Ravi N, Dandekar N, Mysore P, Littman ML (2005) Activity recognition from accelerometer data. AAAI 5:1541–1546
22. Hanai Y, Nishimura J, Kuroda T (2009) Haar-like filtering for human activity recognition using 3d accelerometer. In: Digital signal processing workshop and 5th IEEE signal processing education workshop, 2009. DSP/SPE 2009. IEEE 13th, IEEE, New York, pp 675–678
23. Banos O, Damas M, Pomares H, Rojas I (2013) Handling displacement effects in on-body sensor-based activity recognition. In: International workshop on ambient assisted living. Springer, Heidelberg, pp 80–87
24. Banos O, Toth MA, Damas M, Pomares H, Rojas I (2014) Dealing with the effects of sensor displacement in wearable activity recognition. Sensors 14:9995–10023
25. Punchoojit L, Hongwarittorrn N (2015). A comparative study on sensor displacement effect on realistic sensor displacement benchmark dataset. In: Recent advances in information and communication technology 2015. Springer, New York, pp 97–106
26. Banos O, Galvez JM, Damas M, Pomares H, Rojas I (2014) Window size impact in human activity recognition. Sensors 14:6474–6499
27. Reyes-Ortiz JL, Oneto L, Samá A, Parra X, Anguita D (2016) Transition aware human activity recognition using smartphones. Neurocomputing 171:754–767
28. Breiman L (2001) Random forests. Mach Learn 45:5–32
29. Cox DR, Hinkley DV (1974) Theoretical statistics. Chapman & Hall, London
30. Roggen D, Calatroni A, Rossi M, Holleczek T, Forster K, Tröster G, Lukowicz P, Bannach D, Pirkl G, Ferscha A, et al (2010) Collecting complex activity datasets in highly rich networked sensor environments. In: 2010 seventh international conference on networked sensing systems (INSS). IEEE, New York, pp 233–240
31. Chavarriaga R, Sagha H, Calatroni A, Digumarti ST, Tröster G, Millán JDR, Roggen D (2013) The OPPORTUNITY challenge: a benchmark database for on-body sensor-based activity recognition. Pattern Recogn Lett 34:2033–2042